Desalination and Water Treatment
www.deswater.com

doi: 10.1080/19443994.2015.1123192

57 (2016) 21534–21544
September

Taylor & Francis
Taylor & Francis Group

UV-irradiated carbon nanotubes synthesized from fly ash for adsorption of congo red dyes in aqueous solution

Numan Salah[a,*], Sami S. Habib[a], Zishan H. Khan[b], Rajeev Kumar[c], M.A. Barakat[c]

[a]*Center of Nanotechnology, King Abdulaziz University, Jeddah 21589, Saudi Arabia, Tel. +966 126951595; Fax: +966 126951566; emails: nsalah@kau.edu.sa (N. Salah), sami_habib@hotmail.com (S.S. Habib)*
[b]*Department Appl. Science & Humanities, Jamia Millia Islamia, New Delhi 110025, India, email: zishan_hk@yahoo.co.in*
[c]*Faculty of Meteorology, Environment and Arid Land Agriculture, Department of Environmental Sciences, King Abdulaziz University (KAU), Jeddah 21589, Saudi Arabia, emails: olifiaraju@gmail.com (R. Kumar), mabarakat@gmail.com (M.A. Barakat)*

Received 16 March 2015; Accepted 12 November 2015

ABSTRACT

In this work, carbon nanotubes (CNTs) were synthesized from fly ash and used as adsorbent for the removal of congo red (CR) dye from aqueous solution. The as-synthesized CNTs were exposed to UV radiation for improving the adsorption of dye. The produced nanotubes were characterized by the scanning electron microscopy, transmission electron microscope, X-ray photoelectron spectroscopy, and Raman and FTIR spectroscopies. UV irradiation was found to be an effective tool for enhancing intensity of the observed functional groups and could induce extra defects on the sidewalls of the CNTs. The obtained results show that the adsorption of CR increases from 9.1 to 26.5 mg g^{-1} with increasing the UV irradiation time from 0 to 30 min and maximum adsorption was found to be at pH 4.5. The adsorption efficiency of the UV-irradiated CNTs was decreased from 99.14 to 53.5% by increasing the initial dye concentration from 5 to 50 mg L^{-1}. Langmuir and Freundlich models were fitted to the adsorption equilibrium data and the results reveled that the adsorption of CR onto the CNTs followed the Langmuir isotherm and the maximum monolayer adsorption capacity was found to be 25.61 mg g^{-1}. The results suggest that the synthesized CNTs, which contain naturally exist active groups, besides those induced by the UV irradiation, might be useful for the removal of CR and other water pollutants.

Keywords: Carbon nanotubes; Fly ash; Water pollutants; Congo red; UV irradiation

1. Introduction

In the last decades, carbon nanotubes (CNTs) have drawn much attention due to their unique properties [1,2]. The CNTs consist graphite sheets wrapped into hollow cylinders consisting of single or many layers with diameter ranges from a few to hundreds of nanometers. Several methods were developed in order to produce CNTs [3–11]. However, CNTs' production rates using previously reported methods are still limited due to the high cost of CNTs synthesis. The raw materials, particularly the catalysts and precursors of CNTs, are still costly.

Fly ash is a by-product that generates from various sources such as coal combustion or heavy/crude oil as a fuel mainly in power plants. The ash is often considered as a hazardous waste material that possesses

*Corresponding author.

serious environmental issues. Several studies have proposed ways to utilize the fly ash, thereby decreasing waste and amount in landfills, which could avoid serious environmental challenges [12–15]. Recently, Salah et al. have produced CNTs using carbon-rich fly ash as a source of precursor and catalyst [16,17]. This method seems to be a promising choice for mass production of the CNTs at a very low cost. It also offers a solution for reducing the landfilled fly ash.

The CNTs normally need to be functionalized, which is an essential condition for improving the solubility and dispersion of the CNTs in solutions and incorporating them in new hybrid materials [18,19]. The functional groups attached on the sidewalls of the CNTs carbon surface were found to be responsible for various properties of the matter. These mainly include physicochemical and catalytic properties. Such functional group could be induced by different methods. The most common methods are chemical [20], mechanical [21], and electrochemical methods [22]. However, these methods have drawbacks such as (i) need long time, (ii) consume high amount of chemicals and energy, and (iii) effect the CNTs properties. On the other hand, the UV irradiation is a powerful tool used in many applications like sterilization and disinfection, air purification, polymer processing and modifications, etc. The use of this tool in surface grafting of polymers for the functionalization of graphene sheets along with graphene oxide reduction was also reported [23,24]. In the present work, the CNTs produced from the fly ash were exposed to UV radiation and evaluated for their application in the adsorption of congo red dye.

Congo red (CR) is a synthetic benzidine-based azo dye and is difficult to biodegrade due to its complex aromatic structures. The major sources of this pollutant are textile, printing, paper, and leather industries [25]. A large number of research works have been reported on different materials for the adsorption of CR from aqueous solution [26–28]. However, there is no report on a low-cost material that has the capability of complete adsorption of CR. Some of the proposed materials that showed a good result are very costly. For example, Pal and Deb [26] have reported on the removal of CR dye by the adsorption on coinage nanoparticles (silver nanoparticles and gold nanoparticles) coated activated carbon (AC). They reported that 88.0% of the CR was effectively removed from aqueous solution using gold nanoparticles beads as the adsorption process. Moreover, the use of the CNTs for the removal of CR is rarely appeared. Few reports have studied the removal of other pollutants using CNTs, like Jafari and Aghamiri [29], who reported on the evaluation of the CNTs as a solid-phase extraction sorbent for the removal of cephalexin from aqueous solution.

In the present work, the CNTs produced from carbon-rich fly ash were evaluated for the adsorption of CR from aqueous solution. The nanomaterials were characterized by different techniques including scanning electron microscopy (SEM), transmission electron microscope (TEM), X-ray photoelectron spectroscopy (XPS), Raman spectroscopy, and FTIR spectroscopy. Samples from these CNTs were irradiated by a high-intensity UV light for different times. The adsorption kinetics and isotherm studies were also performed

2. Materials and methods

2.1. Syntheses and characterization of CNTs

Fly ash powder sample was obtained from a water desalination plant in Jeddah, Saudi Arabia. The CNTs were synthesized from the ash using the method described by Salah et al. [17]. The as-produced samples were characterized by a field emission scanning electron microscopy (FESEM), JSM-7500 F (JEOL—Japan) operated at 15 kV. They were also characterized by a high-resolution TEM (using Titan 80, 300 kv (st), FEI). XPS measurement was performed by utilizing a PHI 5000 VersaProbe, Japan, in the range of 275–290 eV. The obtained curve was fitted using *Multipack v8.2c* data analysis software provided with the PHI 5000 VersaProbe ESCA instrument that made use of a combination of Gaussian–Lorentzian peaks. Raman spectra were measured using a DXR Raman microscope, Thermo Scientific, using a 532-nm laser as the excitation source at 6 mW power. FTIR spectra were measured using Thermo Scientific Nicolet IS10 FT-IR spectrometer.

2.2. Adsorption studies

Batch adsorption studies were performed by taking 0.02 g of CNTs in 20 mL of dye solution at a fixed temperature and concentration. The effect of solution pH was studied by preparing various solution pHs range from 4.5 to 9 in flasks containing 20 ml dye solution of 50 mg L^{-1} concentration. The solution pH was adjusted using 0.1 N HCl and 0.1 N NaOH. Then, 0.02 g of UV-irradiated CNTs was added to each flask followed by sonication for 3 h at 30°C. Kinetic study was performed in a series of conical flasks by adding 0.02 g CNTs in 20 mL dye solution of 50 mg L^{-1} concentration at pH 4.5 and 30°C. The solutions were sonicated for the fixed time from 5 to180 min. For the equilibrium isotherm studies, the adsorption was performed by adding 0.02 g adsorbent into 20 mL CR

solution with a concentration ranges from 5 to 50 mg L^{-1} at 30°C for 3 h. After adsorption, the dye solution was filtered through 0.22-μm pore size membrane filter to eliminate the CNTs from solution and the amount of dye remains in the solution was determined by HACH LANGE DR 6000 UV–vis spectrophotometer at 495 nm. The adsorption capacity of UV-irradiated CNTs for the CR was calculated using the following equation:

$$q_e = (C_0 - C_e)V/m \quad (1)$$

where q_e is the amount of CR adsorbed per unit mass of fiber (mg g^{-1}), C_0 and C_e are the initial and equilibrium CR concentrations (mg L^{-1}), respectively, V is the volume of CR solution (L), and m is the mass of the CNTs (g).

2.3. Surface charge determination

Series of conical flasks were prepared for the determination of point of zero charge (pH_{pzc}) of the CNTs. Each flask contains 20 ml of 0.1 M KCl aqueous solution and the pH of the solution was adjusted between 2 and 11 using 0.1 M HCl or 0.1 M NaOH. Thereafter, 0.02 g UV-irradiated (30 min) CNTs were dispersed into each flask and shaked for 24 h in water bath shaker at 30°C. The final pH (pH_f) of the solution was recorded and a graph was plotted between initial pH (pH_i) vs. difference in the initial and final pH ($\Delta pH = pH_i - pH_f$) for the determination of pH_{pzc}.

3. Results and discussion

3.1. CNTs characterization

Fig. 1 shows SEM images ((a) and (b)) at different magnifications for the CNTs produced using carbon-rich fly ash. The images shows well-defined CNTs interim of uniformity, diameters, and lengths. The length of the obtained CNTs is in the micrometer range and the diameter is in the range of 20–40 nm. The figure (inset) shows SEM image for carbon-rich fly ash that could be used to grow CNTs. Fig. 2 shows transmission electron microscopy images ((a) and (b)) for the as-grown CNTs. These images clearly show the CNTs along with some catalyst particles (Fig. 2(a)). A high-resolution TEM image (Fig. 2(b)) shows the multi-layered structure indicating that the synthesized tubes are multiwalled carbon nanotubes (MWCNTs). This image shows nanotube with 11 inner and outer walls. The thickness of each wall is around 0.35 nm. These results are similar to that reported earlier by Salah et al. [17].

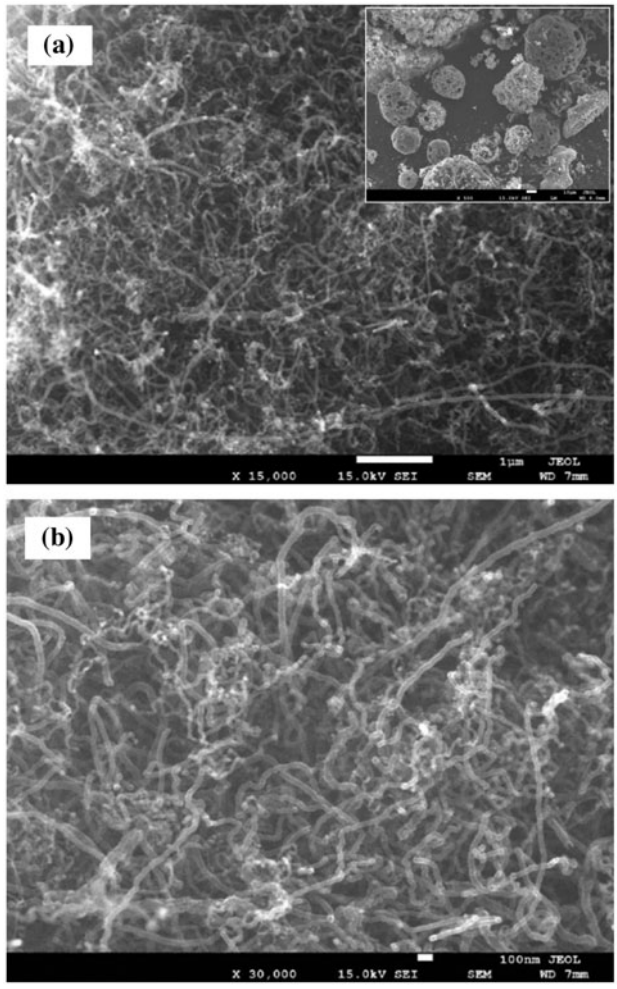

Fig. 1. SEM images at different magnification of the as-grown CNTs samples produced using fly ash. The figure in the inset is SEM image for carbon-rich fly ash used to grow CNTs.

XPS spectrum of the as-produced CNTs is presented in Fig. 3. The figure shows the peaks of sp^2 and sp^3 carbons [30]. The intensity ratio of sp^2/sp^3 carbons is around 7.5 eV. Deconvolution of this spectrum results in other two bands located at 288.2 and 290.5 eV. The first one might be assigned to –COO (carboxyls, carboxylic anhydrides, and esters), while the second one at 290.5 eV is π–π^* transition carbon (shakeup carbon in aromatic compounds) or COOH group [31]. These groups might be quite useful for the application of the produced nanotubes as an adsorbent for organic pollutants.

Raman spectra of un-irradiated and UV-irradiated CNTs are shown in Fig. 4. The spectrum of un-irradiated CNTs (curve *a*) clearly shows graphite (G) and defect (D) bands at around 1,585 and 1,350 cm^{-1}

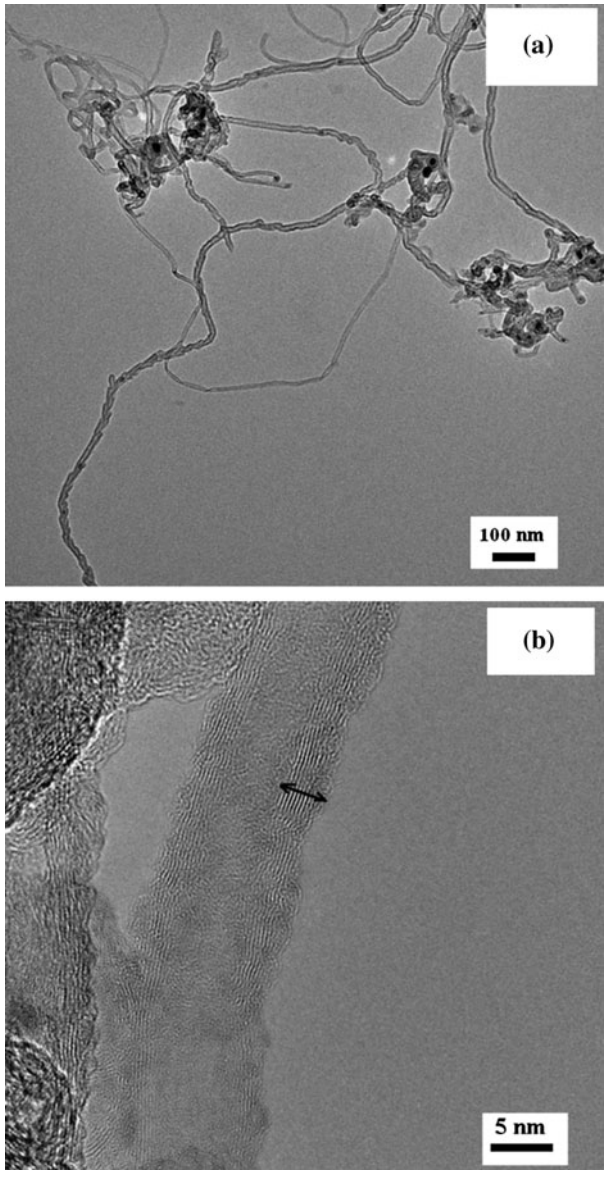

Fig. 2. (a) TEM image and (b) high-resolution TEM image for the as-grown CNT samples produced using fly ash.

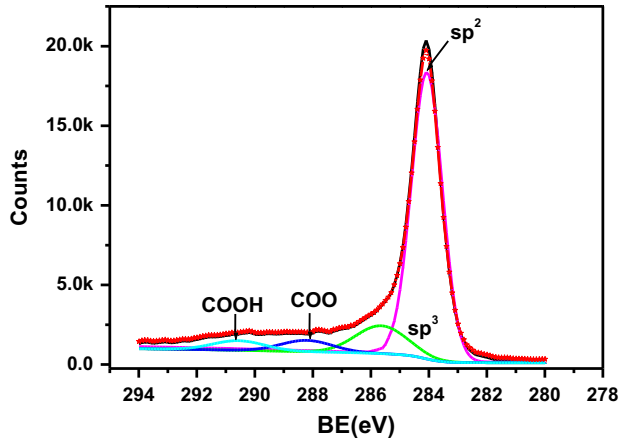

Fig. 3. XPS spectrum of the as-grown CNT samples produced using fly ash.

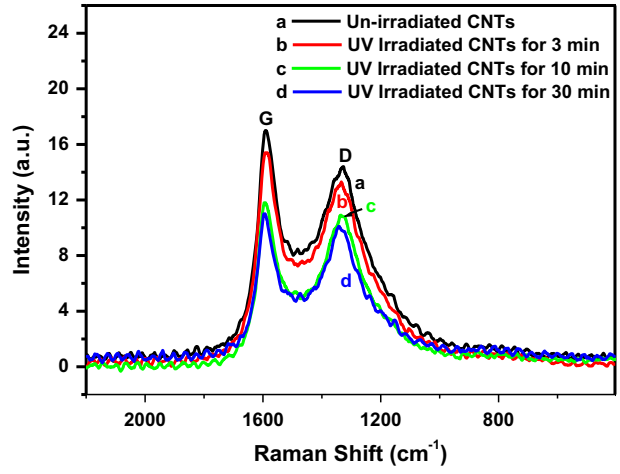

Fig. 4. Raman spectra of un-irradiated and UV-irradiated CNTs for different times.

[31,32]. The intensity ratio of the D and G bands (I_D/I_G) is often used as an indication of the level of defect density on a graphitic carbon sample [33]. The intensity ratio of G to D bands in the present CNTs is around 1.2. However, the intensity and intensity ratio of UV-irradiated samples were observed to vary (curves b–d). By increasing the irradiation time, the intensity of G band is significantly decreased. This indicates that a major modification is induced in the surface of the irradiated nanotubes.

Fig. 5 shows FTIR spectra of both un-irradiated and UV-irradiated CNTs. The spectrum of un-irradiated CNTs (curve a) shows major peaks at 2,900–2,970, 1,723, and 1,527 cm^{-1} besides smaller one at 1,461, 1,327, 1,299, 1,261 and 1,175 cm^{-1}. FTIR spectra of the UV-irradiated CNTs show similar, but enhanced bands along with emergence of extra peaks located at 2,353–2,360 cm^{-1} (curves b–e). The broad peak at 2,900–2,970 cm^{-1} might be ascribed to the asymmetric and symmetric stretching vibration of C–H side chain group of the aromatic ring [34]. The second band at 1,723 cm^{-1} might be assigned to carbonyl (C=O) stretching vibration of carboxyl groups [35], while that at 1,527 cm^{-1} is the carbon double bonding (C=C) [34]. The two broad peaks located at 2,330 and 2,360 cm^{-1}, induced in the irradiated samples, might be due to the atmospheric CO_2 adsorbed on the sidewall of these irradiated CNTs [36,37].

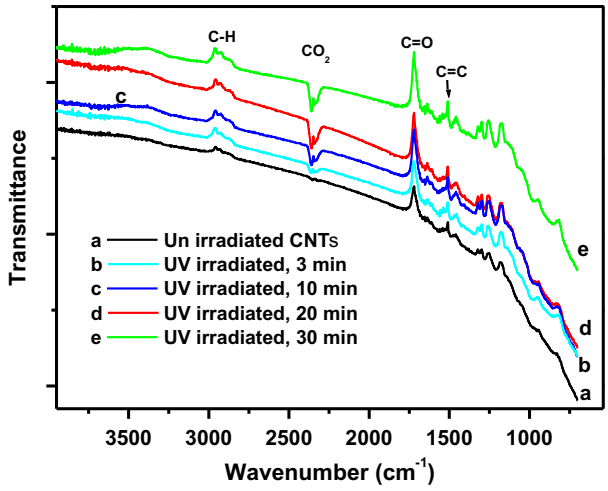

Fig. 5. FTIR spectra of un-irradiated and UV-irradiated CNTs for different times.

3.2. Adsorption of CR dye on the synthesized CNTs

3.2.1. Effect of UV irradiation time

The effect of UV irradiation time onto the CNTs was studied to optimize the effectiveness of adsorbent. The CNT samples were irradiated for 3, 10, 20, and 30 min under UV light and the adsorption efficiency of the irradiated CNTs was evaluated for the removal of CR. As shown in Fig. 6, the adsorption capacity of the CNTs for the CR increased with increasing the UV exposure time from 3 to 30 min. This might be attributed to the fact that higher irradiation time could possibly produce more defect and oxygenous functional groups on the surface of the CNTs, which favor the adsorption of dye [38]. Therefore, the CNTs irradiated for 30 min under UV light were used for the brief adsorption experiments.

3.2.2. Effect of solution pH and adsorption mechanism

Congo red is a highly pH sensitive dye, which shows structural and color changes with the change in the solution pH. In acidic solution (pH < 3), the CR turns to blue color due to the ammonium–azonium tautomerism, while in neutral and basic medium (pH > 5), the CR retains its original red color [39,40]. Therefore, the effect of solution pH was studied on the pH ranges from 4.5 to 9 as shown in Fig. 7. The adsorption of CR decreases with the increase in solution pH; the maximum adsorption was found at pH 4.5. The adsorption mechanism can be explained on the basis of surface chemistry of the CNTs and CR. The point of zero charge of the CNTs was found to be 4.7. The surface charge of the CNTs is positive when the solution pH is lower than 4.7. The CR is a negatively charged acidic dye having two sulfonate groups ($-SO_3^-Na^+$). At low pH, negatively charged CR molecules attracted electrostatically with positively charged oxidized CNTs ($CNTs{-}OH_2^+ + {-}SO_3^- \rightarrow CNTs{-}OH_2^+{-}{}^-O_3S{-}$) [39–41]. On increasing the solution pH, the CR adsorption decreases through deprotonation of oxygenous functional groups of the CNTs (over pH_{pzc}). This is due to the electrostatic repulsion between the negatively charged adsorbent surface and the CR ($CNTs{-}O^- + {-}SO_3^- \rightarrow CNTs{-}O^- \leftrightarrow {}^-O_3S{-}$) [39–41]. However, a slight adsorption was observed at higher pH which may be attributed to the synergetic

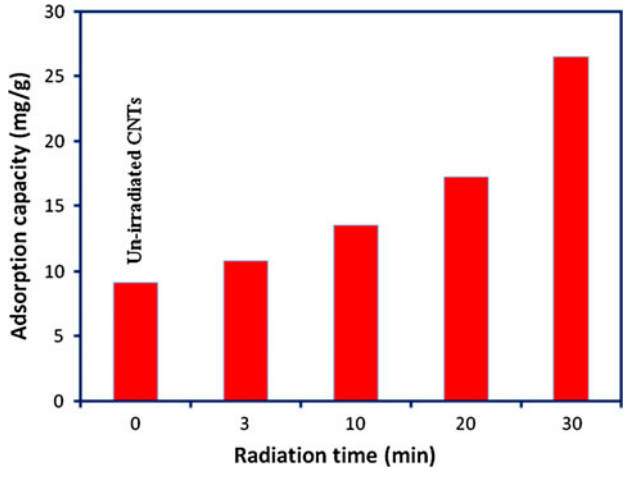

Fig. 6. Effect of UV irradiation time on adsorption of CR dye.

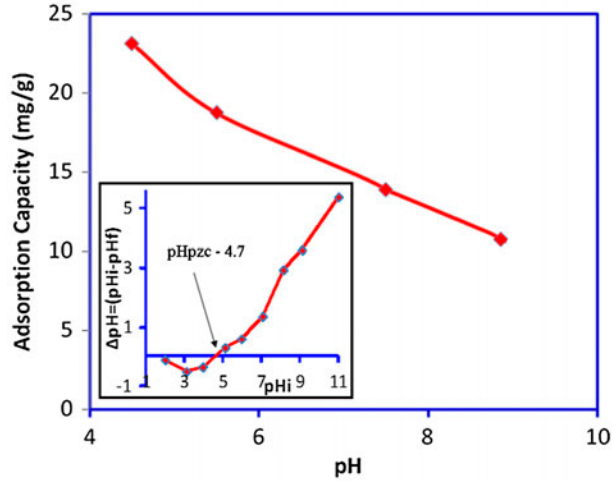

Fig. 7. Effect of solution pH on CR adsorption onto UV-irradiated CNTs (inset: plot for pH_{pzc} determination).

effect of π–π interactions, hydrogen bonding, and van der Waals forces exist between the irradiated CNTs and CR molecules [42]. The presence of oxygenous functional groups such as carboxylic group (–COOH) and hydroxyl group (–OH) have been confirmed by the FTIR and XPS studies of the CNTs. These oxygenous functional groups of adsorbent and amine, sulfonate groups of the CR dye are expected to be mainly involved in the adsorption at solid–solution interface. The following adsorption mechanisms can be expected between irradiated CNTs and CR molecules [43]: (i) hydrogen bonding between the nitrogen and oxygen atoms containing functional groups of adsorbent and adsorbate, (ii) π–π interaction between the aromatic ring of the CNTs and CR molecules, and (iii) hydrophobic interaction—the sidewall of the CNTs are highly hydrophobic due to high π electron density of sp^2 carbons, which may interact with the CR through hydrophobic interaction. A schematic illustration of the possible interaction between the CR and irradiated CNTs is shown in Fig. 8.

3.2.3. Kinetics study

The attainment of CR adsorption equilibrium onto the CNTs is shown in Fig. 9. It can be seen that the sharp increase in the CR adsorption with the increase in contact time and equilibrium was established within 2 h. Initially, fast adsorption of CR was may be due to the adsorption on the vacant active surface sites and, thereafter, equilibrium was established due to saturation of active sites [44]. Moreover, to find the rate for the CR adsorption onto the CNTs, pseudo-first [45]- and pseudo-second-order kinetic [46] models were applied. The pseudo-first- and pseudo-second-order kinetic equations in linear form are:

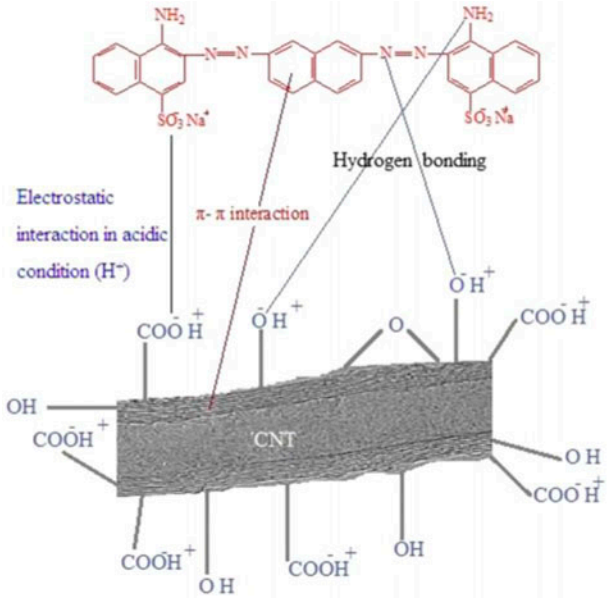

Fig. 8. Schematic illustration of the possible interaction between CR and irradiated CNTs.

$$\log \frac{q_e}{q_t} = \log - \frac{k_1}{2.303} t \quad (2)$$

$$\frac{t}{q_t} = \frac{1}{k_2 q_e^2} + \frac{t}{q_e} \quad (3)$$

where k_1 is the pseudo-first-order rate constant (min^{-1}), q_e (mg g^{-1}) and q_t (mg g^{-1}) are the CR adsorption capacity at equilibrium and after time t (min), respectively, k_2 is the pseudo-second-order rate constant (g mg^{-1} min^{-1}). The values of the pseudo-first-order and pseudo-second-order kinetic parameters were calculated from the plots $\log(q_e - q_t)$ vs. t and t/q_e vs. t, respectively. From the values in Table 1, the calculated adsorption capacity (q_e^{cal}) for the pseudo-second-order kinetic equation is much close to the experimental CR adsorption capacity (q_e^{exp}) than the pseudo-first-order kinetic equation, indicating the fitness of the pseudo-second order to the experimental adsorption data. Moreover, the value of R^2 for the pseudo-second-order equation is much higher than the pseudo-first-order equation, confirming the suitability of the pseudo-second-order kinetic model to describe the CR adsorption onto the CNTs [47]. Furthermore, to determine the mass transfer rate of the CR from solution to CNTs, Weber–Morris intra-particle diffusion model [48] was applied:

Table 1
Kinetic parameters for the removal of CR onto UV-irradiated MWCNTs

Parameters	Values
$q_e^{(exp)}$ (mg g^{-1})	25
Pseudo-first-order kinetic model	
$q_e^{(cal)}$ (mg g^{-1})	37.385
k_1 (min^{-1})	0.00368
R^2	0.8108
Pseudo-second-order kinetic model	
$q_e^{(cal)}$ (mg g^{-1})	27.100
k_2 (g mg^{-1} min^{-1})	0.00316
R^2	0.9985

$$q_t = k_{id} t^{1/2} + C \quad (4)$$

where k_{id} (g mg^{-1} min$^{-1/2}$) and C (mg g^{-1}) are the intra-particle diffusion rate coefficient and constant related to the thickness of the boundary layer, respectively. A plot for the intra-particle diffusion with two curved portions is show in Fig. 9 (inset). The first straight portion indicates the adsorption of CR onto the surface of the CNTs, while the second portion indicates the attainment of equilibrium. These results revalued that the CR adsorbed onto the CNTs through boundary layers diffusion [44].

3.2.4. Adsorption isotherm studies

The efficiency of the UV-irradiated CNTs decreased from 99.14 to 53.5% with increasing the initial dye concentration from 5 to 50 mg L^{-1} as shown in Fig. 10. This was obvious because the numbers of active sites for the adsorption are constant while the concentration of the CR in solution increases. Therefore, after equilibrium attainment, uptake of the dye decreased. For better understanding of the distribution of the CR molecules between the solution and solid phase, isotherm models, namely Langmuir, Freundlich, and Temkin, were used to fit the adsorption equilibrium data. The Langmuir isotherm model [49] is valid for the monolayer adsorption onto adsorbent surface, which contains finite number of identical

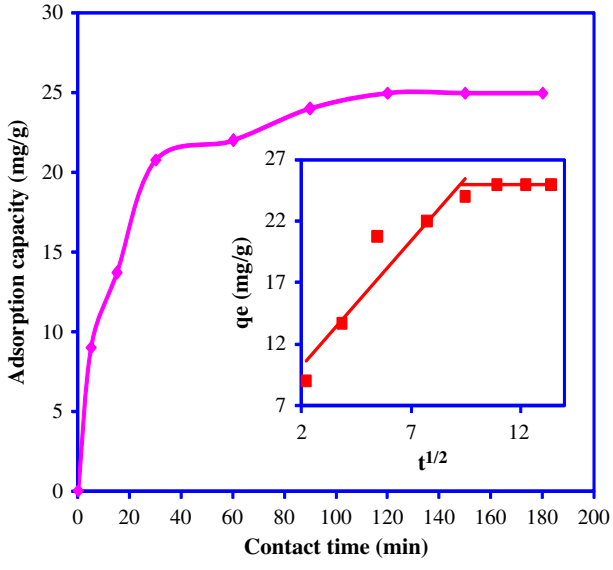

Fig. 9. Effect of contact time on CR adsorption UV-irradiated CNTs (inset: Weber–Morris plot).

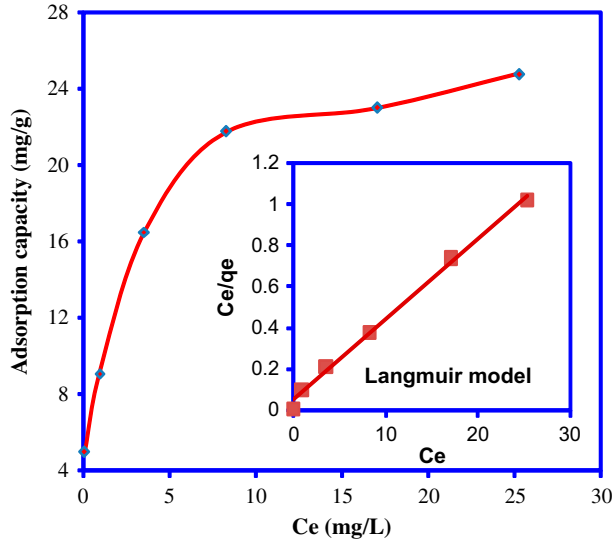

Fig. 10. Adsorption isotherm plot for CR adsorption UV-irradiated CNTs (inset: Langmuir isotherm plot).

active sites and there is no transmigration of the adsorbate in the plane of the surface. The linear equation for the Langmuir isotherm is as follows:

$$\frac{C_e}{q_e} = \frac{1}{q_m b C_e} + \frac{C_e}{q_m} \quad (5)$$

where q_e (mg g^{-1}) is the amount of CR molecules adsorbed at equilibrium, C_e (mg L^{-1}) is the equilibrium concentration of CR, q_m (mg g^{-1}) is the maximum monolayer adsorption capacity, and b (L mg^{-1}) is the adsorption equilibrium constant. The values of the Langmuir isotherm constants were calculated from plot of C_e/q_e vs. C_e.

The Freundlich isotherm model [50] assumes that the adsorption of adsorbate species takes place through multilayer and heterogeneous system, characterized by the heterogeneity factor $1/n$. The linear equation for the Freundlich isotherm is as follows:

$$\ln q_e = \ln K_F + \frac{1}{n} \ln C_e \quad (6)$$

where K_F and n are the Freundlich constants, which indicate the adsorption capacity and adsorption intensity. The values of the Freundlich isotherm parameters were calculated from plot of ln q_e vs. ln C_e.

The Temkin isotherm model [51] is based on the adsorbent–adsorbate interactions and along with the saturation of adsorbent active sites, the adsorption

Table 2
Adsorption isotherm parameters for the removal of CR onto UV-irradiated MWCNTs

Langmuir isotherm model			Freundlich isotherm model			Temkin isotherm model		
q_m (mg g^{-1})	b (L mg^{-1})	R^2	K_F ($mg^{1-1/n}$ $L^{1/n}$ g^{-1})	n	R^2	A (L mg^{-1})	B	R^2
25.64	0.740	0.995	10.990	3.745	0.975	48.589	3.287	0.928

Table 3
Adsorption capacities of various adsorbents used for the removal of congo red

Adsorbent	Adsorption capacity (mg g^{-1})	Refs.
AgNPs-coated AC	64.8	[26]
AuNPs-coated AC	74.05	[26]
Bael shell carbon	98.03	[40]
Graphene oxide/chitosan/silica nanocomposite	294.12	[41]
Rice husk ash	7.047	[52]
Polypyrrole–polyaniline nanofibers	222.22	[53]
Coir pith carbon	6.7	[54]
Fe_3O_4@graphene nanocomposite	33.66	[55]
Rice bran	14.6	[56]
Bentonite	19.9	[57]
4-Vinyl pyridine-grafted poly(ethyleneterephthalate) fibers	18.1	[58]
Activated carbon (Laboratory grade)	1.88	[59]
Bagasse fly ash	11.89	[59]
Montmorillonite	12.70	[60]
Sugarcane bagasse	38.2	[61]
PVC	10.75	[62]
PVC-GN	27.027	[62]
pTSA–Pani@GN–PVC	45.454	[62]
PVC@GN-Pani-*b*	26.315	[63]
PVC@GN-Pani-*a*	31.250	[63]
PVC@GN-Pani-*s*	40.00	[63]
CNTs	25.64	This study

energy decreases linearly rather than decreasing exponentially. The linear equation for the Temkin isotherm model is:

$$q_e = B \ln A + B \ln C_e \quad (7)$$

where A and B are the Temkin isotherm parameters, related to the equilibrium binding constant (L mg^{-1}) and the heat of adsorption (kJ mol^{-1}), respectively. The values of the Temkin constants were calculated from plot of q_e vs. ln C_e.

The values of the adsorption isotherm parameters and constants, calculated from their respective plots, are mentioned in Table 2. It is clear that the Langmuir model shows better fit with the experimental equilibrium data than the Freundlich and Temkin isotherm models. A value of higher correlation coefficient (R^2: 0.995) was obtained for the Langmuir equation in contrast to the Freundlich (R^2: 0.975) and Temkin (R^2: 0.928) isotherm equations [41,42]. The maximum monolayer adsorption capacity of UV-irradiated CNTs was found to be 25.64 mg g^{-1}. Table 3 summarizes the adsorption capacity of various kinds of materials used for the removal of CR from aqueous solution and it can be seen from Table 3 that UV-treated CNTs have shown a better adsorption same as the previously reported adsorbent.

4. Conclusions

The CNTs were synthesized from carbon-rich fly ash and successively evaluated for the adsorption of congo red dye in aqueous solution. These CNTs were found to have active carboxyl groups on their sidewalls, besides extra defects formed by the UV irradiation. The obtained results showed that the adsorption

of CR increased by increasing UV irradiation time to the CNTs, but it decreased with increasing initial dye concentration. The Langmuir isotherm model is found to fit well with the adsorption experimental results. The produced nanomaterials with their naturally exist active groups, besides those induced by the UV irradiation, might be successively applied for the removal of CR dye and other organic pollutants.

Acknowledgments

This project was funded by the National Plan for Science, Technology and Innovation (MAARIFAH), King Abdulaziz City for Science and Technology, the Kingdom of Saudi Arabia, Award No. (10-NAN1104-03). The authors also, acknowledge with thanks Science and Technology Unit, King Abdulaziz University for technical support.

References

[1] M.M.J. Treacy, T.W. Ebbesen, J.M. Gibson, Exceptionally high Young's modulus observed for individual carbon nanotubes, Nature 381 (1996) 678–680.
[2] S.J. Tans, M.H. Devoret, H. Dai, A. Thess, R.E. Smalley, L.J. Geerligs, C. Dekker, Individual single-wall carbon nanotubes as quantum wires, Nature 386 (1997) 474–477.
[3] T.W. Ebbesen, P.M. Ajayan, Large-scale synthesis of carbon nanotubes, Nature 358 (1992) 220–222.
[4] S. Cui, P. Scharff, C. Siegmund, D. Schneider, K. Risch, S. Klötzer, L. Spiess, H. Romanus, J. Schawohl, Investigation on preparation of multiwalled carbon nanotubes by DC arc discharge under N_2 atmosphere, Carbon 42 (2004) 931–939.
[5] K.S. Kim, C.T. Kingston, D. Ruth, M. Barnes, B. Simard, Synthesis of high quality single-walled carbon nanotubes with purity enhancement and diameter control by liquid precursor Ar–H_2 plasma spraying, Chem. Eng. J. 250 (2014) 331–341.
[6] J. Gallego, G. Sierra, F. Mondragon, J. Barrault, C.B. Dupeyrat, Synthesis of MWCNTs and hydrogen from ethanol catalytic decomposition over a Ni/La_2O_3 catalyst produced by the reduction of $LaNiO_3$, Appl. Catal. A: Gen. 397 (2011) 73–81.
[7] A.A. Stramel, M.C. Gupta, H.R. Lee, J. Yu, W.C. Edwards, Pulsed laser deposition of carbon nanotube and polystyrene–carbon nanotube composite thin films, Opt. Lasers Eng. 48 (2010) 1291–1295.
[8] F. Kokai, I. Nozaki, T. Okada, A. Koshio, T. Kuzumaki, Efficient growth of multi-walled carbon nanotubes by continuous-wave laser vaporization of graphite containing B_4C, Carbon 49 (2011) 1173–1181.
[9] A.R. John, P. Arumugam, Studies on structural and magnetic properties of pristine and nickel-filled carbon nanotubes synthesized using $LaNi_5$ alloy particles as a catalyst, Chem. Eng. J. 243 (2014) 436–447.
[10] A. Lo, N. Yu, S. Huang, C. Hung, S. Liu, Z. Lei, C. Kuo, S. Liu, Fabrication of CNTs with controlled diameters and their applications as electrocatalyst supports for DMFC, Diam. Relat. Mater. 20 (2011) 343–350.
[11] J. Zhang, R. Tu, T. Goto, Preparation of carbon nanotube by rotary CVD on Ni nano-particle precipitated cBN using nickelocene as a precursor, Mater. Lett. 65 (2011) 367–370.
[12] J. Li, X. Zhuang, O. Font, N. Moreno, V.R. Vallejo, X. Querol, A. Tobias, Synthesis of merlinoite from Chinese coal fly ashes and its potential utilization as slow release K-fertilizer, J. Hazard. Mater. 265 (2014) 242–252.
[13] A. Mittal, J. Mittal, A. Malviya, D. Kaur, V.K. Gupta, Decoloration treatment of a hazardous triarylmethane dye, Light Green SF (Yellowish) by waste material adsorbents, J. Colloid Interface Sci. 342 (2010) 518–527.
[14] V.L. Markad, K.M. Kodam, V.S. Ghole, Effect of fly ash on biochemical responses and DNA damage in earthworm, *Dichogaster curgensis*, J. Hazard. Mater. 215–216 (2012) 191–198.
[15] A. Mittal, D. Kaur, A. Malviya, J. Mittal, V.K. Gupta, Adsorption studies on the removal of coloring agent phenol red from wastewater using waste materials as adsorbents, J. Colloid Interface Sci. 337 (2009) 345–354.
[16] N. Salah, S.S. Habib, Z.H. Khan, A. Memic, M.N. Nahas, Growth of Carbon Nanotubes on catalysts obtained from carbon rich fly ash, Digest J. Nanomater. Biostruc. 7 (2012) 1279–1288.
[17] N. Salah, S.S. Habib, Z.H. Khan, A.A. Al-ghamdi, A. Memic, Formation of carbon nanotubes from carbon rich fly ash: Growth parameters and mechanism, Mater. Manuf. Process. 31 (in press) 146–156.
[18] A. Hirsch, Functionalization of single-walled carbon nanotubes, Angew. Chem. Int. Ed. 41 (2002) 1853–1859.
[19] T.A. Saleh, V.K. Gupta, Column with CNT/magnesium oxide composite for lead(II) removal from water, Environ. Sci. Pollut. Res. 19 (2012) 1224–1228.
[20] F. Xie, J. Phillips, I.F. Silva, M.C. Palma, J.A. Menéndez, Microcalorimetric study of acid sites on ammonia- and acid-pretreated activated carbon, Carbon 38 (2000) 691–700.
[21] J.P. Boudou, J.I. Paredes, A. Cuesta, A. Martínez-Alonso, J.M.D. Tascón, Oxygen plasma modification of pitch-based isotropic carbon fibres, Carbon 41 (2003) 41–56.
[22] C.C. Hu, C.C. Wang, Effects of electrolytes and electrochemical pretreatments on the capacitive characteristics of activated carbon fabrics for supercapacitors, J. Power Sources 125 (2004) 299–308.
[23] I. Roppolo, A. Chiappone, K. Bejtka, E. Celasco, A. Chiodoni, F. Giorgis, M. Sangermano, S. Porro, A powerful tool for graphene functionalization: Benzophenone mediated UV grafting, Carbon 77 (2014) 226–235.
[24] Y.H. Ding, P. Zhang, Q. Zhuo, H.M. Ren, Z.M. Yang, Y. Jiang, A green approach to the synthesis of reduced graphene oxide nanosheets under UV irradiation, Nanotechnology 22 (2011) 215601.
[25] R. Han, D. Ding, Y. Xu, W. Zou, Y. Wang, Y. Li, L. Zou., Use of rice husk for the adsorption of congo red from aqueous solution in column mode, Bioresour. Technol. 99 (2008) 2938–2946.
[26] J. Pal, M.K. Deb, Efficient adsorption of congo red dye from aqueous solution using green synthesized

coinage nanoparticles coated activated carbon beads, Appl. Nanosci. 4 (2014) 967–978.
[27] V.K. Gupta, I. Ali, T.A. Saleh, A. Nayak, S. Agarwal, Chemical treatment technologies for waste-water recycling—An overview, RSC Adv. 2 (2012) 6380–6388.
[28] T. Feng, S. Xiong, F. Zhang, Application of cross-linked porous chitosan films for Congo red adsorption from aqueous solution, Desalin. Water Treat. 53 (2015) 1970–1976.
[29] M. Jafari, S.F. Aghamiri, Evaluation of carbon nanotubes as solid-phase extraction sorbent for the removal of cephalexin from aqueous solution, Desalin. Water Treat. 28 (2011) 55–58.
[30] P. Chu, L. Li, Characterization of amorphous and nanocrystalline carbon films, Mater. Chem. Phys. 96 (2006) 253–277.
[31] Y.K. Kim, H. Park, Light-harvesting multi-walled carbon nanotubes and CdS hybrids: Application to photocatalytic hydrogen production from water, Energy Environ. Sci. 4 (2011) 685–694.
[32] D.Q. Yang, J.F. Rochette, E. Sacher, Functionalization of multiwalled carbon nanotubes by mild aqueous sonication, J. Phys. Chem. B 109 (2005) 7788–7794.
[33] C.V. Vix-Guterl, M. Couzi, J. Dentzer, Surface characterizations of carbon multiwall nanotubes: Comparison between surface active sites and Raman spectroscopy, J. Phys. Chem. B 108 (2004) 19361–19367.
[34] R. Yudianti, H. Onggo, Sudirman, Y. Saito, T. Iwata, J. Azuma, Analysis of functional group sited on multiwall carbon nanotube surface, Open Mater. Sci. J. 5 (2011) 242–247.
[35] S.Y. Lee, S.J. Park, Hydrogen adsorption of acid-treated multi-walled carbon nanotubes at low temperature, Bull. Korean Chem. Soc. 31 (2010) 1596–1600.
[36] X. Feng, C. Matranga, R. Vidic, E. Borguet, A vibrational spectroscopic study of the fate of oxygen-containing functional groups and trapped CO_2 in single-walled carbon nanotubes during thermal treatment, J. Phys. Chem. B 108 (2004) 19949–19954.
[37] Y. Hsieh, Y. Chou, C. Lin, T. Hsieh, C. Shu, Thermal analysis of multi-walled carbon nanotubes by kissinger's corrected kinetic equation, Aerosol Air Qual. Res. 10 (2010) 212–218.
[38] M. Grujicic, G. Cao, A.M. Rao, T.M. Tritt, S. Nayak, UV-light enhanced oxidation of carbon nanotubes, Appl. Surf. Sci. 214 (2003) 289–303.
[39] J. Barkauskas, I. Stankevičienė, J. Dakševič, A. Padarauskas, Interaction between graphite oxide and Congo red in aqueous media, Carbon 49 (2011) 5373–5381.
[40] R. Ahmad, R. Kumar, Adsorptive removal of congo red dye from aqueous solution using bael shell carbon, Appl. Surf. Sci. 257 (2010) 1628–1633.
[41] Q. Du, J. Sun, Y. Li, X. Yang, X. Wang, Z. Wang, L. Xia, Highly enhanced adsorption of congo red onto graphene oxide/chitosan fibers by wet-chemical etching off silica nanoparticles, Chem. Eng. J. 245 (2014) 99–106.
[42] S. Debnath, A. Maity, K. Pillay, Impact of process parameters on removal of Congo red by graphene oxide from aqueous solution, J. Environ. Chem. Eng. 2 (2014) 260–272.
[43] V.K. Gupta, R. Kumar, A. Nayak, T.A. Saleh, M.A. Barakat, Adsorptive removal of dyes from aqueous solution onto carbon nanotubes: A review, Adv. Colloid Interface Sci. 193–194 (2013) 24–34.
[44] R. Kumar, M.O. Ansari, M.A. Barakat, Adsorption of brilliant green by surfactant doped polyaniline/MWCNTs composite: Evaluation of the kinetic, thermodynamic, and isotherm, Ind. Eng. Chem. Res. 53 (2014) 7167–7175.
[45] S. Lagergren, Zur theorie der sogenannten adsorption geloster stoffe (About the theory of so-called adsorption of soluble substances), K. Sven, Vetenskapsakad. Handl. 24 (1898) 1–39.
[46] G. McKay, Y.S. Ho, Pseudo-second order model for sorption processes, Process Biochem. 34 (1999) 451–465.
[47] A. Mittal, J. Mittal, A. Malviya, V.K. Gupta, Adsorptive removal of hazardous anionic dye "Congo red" from wastewater using waste materials and recovery by desorption, J. Colloid Interface Sci. 340 (2009) 16–26.
[48] W.J. Weber Jr., J.C. Morris, Kinetics of adsorption on carbon from solution. J. Sanit. Eng. Div.-ASCE 89 (1963) 31–59.
[49] I. Langmuir, The adsorption of gases on plane surfaces of glass, mica and platinum, J. Am. Chem. Soc. 40 (1918) 1361–1403.
[50] H. Freundlich, Ueber die Adsorption in Loesungen (Over the adsorption in solution), J. Phys. Chem. 57 (1906) 385–470.
[51] M.I. Temkin, V. Pyzhev, Kinetics of ammonia synthesis on promoted iron catalysts, Acta Physiochem. SSR 12 (1940) 217–222.
[52] A.K. Chowdhury, A.D. Sarkar, A. Bandyopadhyay, Rice husk ash as a low cost adsorbent for the removal of methylene blue and congo red in aqueous phases, Clean 37 (2009) 581–581.
[53] M. Bhaumik, R. McCrindle, A. Maity, Efficient removal of Congo red from aqueous solutions by adsorption onto interconnected polypyrrole–polyaniline nanofibres, Chem. Eng. J. 228 (2013) 506–515.
[54] C. Namasivayam, D. Kavitha, Removal of Congo Red from water by adsorption onto activated carbon prepared from coir pith, an agricultural solid waste, Dyes Pigm. 54 (2002) 47–58.
[55] Y.G. Yao, S.D. Miao, S.Z. Liu, L.P. Ma, H.G. Sun, S.B. Wang, Synthesis, characterization, and adsorption properties of magnetic Fe_3O_4@graphene nanocomposite, Chem. Eng. J. 184 (2012) 326–332.
[56] X.S. Wang, J.P. Chen, Biosorption of Congo Red from aqueous solution using wheat bran and rice bran: Batch studies, Sep. Sci. Technol. 44 (2009) 1452–1466.
[57] G.C. Panda, S.K. Das, A.K. Guha, Jute stick powder as a potential biomass for the removal of congo red and rhodamine B from their aqueous solution, J. Hazard. Mater. 164 (2009) 374–379.
[58] M. Arslan, M. Yiğitoğlu, Adsorption behavior of Congo red from an aqueous solution on 4-vinyl pyridine grafted poly(ethylene terephthalate) fibers, J. Appl. Polym. Sci. 107 (2008) 2846–2853.
[59] I.D. Mall, V.C. Srivastava, N.K. Agarwal, I.M. Mishra, Removal of congo red from aqueous solution by bagasse fly ash and activated carbon: Kinetic study and equilibrium isotherm analyses, Chemosphere 61 (2005) 492–501.
[60] L. Wang, A. Wang, Adsorption characteristics of Congo Red onto the chitosan/montmorillonite nanocomposite, J. Hazard. Mater. 147 (2007) 979–985.
[61] Z. Zhang, L. Moghaddam, I.M. O'Hara, W.O.S. Doherty, Congo Red adsorption by ball-milled sugarcane bagasse, Chem. Eng. J. 178 (2011) 122–128.

[62] M.O. Ansari, R. Kumar, N. Parveen, M.A. Barakat, M.H. Cho, Facile strategy for the synthesis of non-covalently bonded and para-toluene sulfonic acid-functionalized fibrous polyaniline@graphene–PVC nanocomposite for the removal of Congo red, New J. Chem. 39 (2015) 7004–7011.

[63] R. Kumar, M.O. Ansari, N. Parveen, M.A. Barakat, M.H. Cho, Simple route for the generation of differently functionalized PVC@graphene–polyaniline fiber bundles for the removal of Congo red from wastewater. RSC Adv. 5 (2015) 61486–61494.